Onset of convection in Soret-driven instability

V. M. Shevtsova, D. E. Melnikov, and J. C. Legros*
MRC, CP-165/62, Université Libre de Bruxelles, 50 av. F.D. Roosevelt, B-1050 Brussels, Belgium
(Received 26 December 2005; published 26 April 2006)

It is common knowledge that light fluids rise while heavy fluids sink in the gravity field. The most obvious case is the isothermal Rayleigh-Taylor instability when a heavy fluid is placed on top of a light one. In the nonisothermal case, while heating from above, the density stratification is stable in a pure liquid. However, unstable density stratification might be established in a binary mixture with a negative Soret effect in the case of heating from above: the heavier liquid is accumulated on the top of the lighter one. Due to the large differences between viscous, thermal, and diffusion times the system has a tendency to fingering buoyant instabilities. At some moment the flow may be initiated. Near the onset of convection the flow pattern has a columnar convective structure: for a relatively low applied temperature difference ΔT the lighter and colder liquid is drawn up in the central part of the cell and the heavier liquid flows down along the walls. For finite size systems the situation is reversed at higher ΔT. Here we present results of three-dimensional direct numerical simulations of heat and mass transfer in a system with a negative Soret effect. While the development of Soret-induced convection is similar for a wide class of liquids: water based mixtures, colloidal, and polymer solutions, the parameters of the chosen system correspond to a realistic binary mixture of water (90%) and isopropanol (10%) enabling comparison of theoretical predictions with planned experimental studies.

DOI: 10.1103/PhysRevE.73.047302 PACS number(s): 47.20.Bp, 47.20.Ky, 47.27−i, 47.35.−i

INTRODUCTION

Mixtures provide a richer variety of bifurcation phenomena and convective states in comparison with single liquids. The heat transfer within a single fluid (conduction or convection) is characterized by the Rayleigh number

$$\mathrm{Ra} = \frac{g\beta_T \Delta T L^3}{\nu\alpha}. \tag{1}$$

In Soret relevant problems in the Rayleigh-Benard (RB) configuration, when the concentration boundary layer has enough time to develop, the threshold condition is characterized by the solutal Rayleigh number

$$\mathrm{Ra}_s = -\frac{\psi}{\mathrm{Le}}\mathrm{Ra}, \tag{2}$$

where $\mathrm{Le}=D/\alpha$ is the Lewis number. Here D is the molecular diffusion and α is the thermal diffusivity. The strength of the Soret effect is described by the separation ratio

$$\psi = C_0(1-C_0)\frac{\beta_C}{\beta_T}S_T \tag{3}$$

which is the ratio of the concentration-induced density gradient to the temperature-induced density gradient in the quiescent state. Externally ψ is controlled by varying the mean temperature and the initial concentration of the mixture. For considered mixture the thermal and solutal expansions β_T and β_C are positive, so the sign of ψ coincide, with the sign of the Soret coefficient S_T. A negative sign of S_T implies that the denser component migrates towards a hot wall (opposite to the buoyancy force).

The threshold conditions for the RB convection in an infinite layer of a single liquid (transition from conductive to convective state) is well known and for perfectly isothermic plates is $\mathrm{Ra}^0=1708$; while $\mathrm{Ra}=720$ for perfectly insulating plates, in both cases of the heat transfer and mass transfer. Thus, $\mathrm{Ra}=720$, in the case of heat insulation and $\mathrm{Ra}_s^0=720$, for a mass impermeability. By choosing a mixture with a large ratio $|\psi/\mathrm{Le}|$ one may study the solutal convection at subcritical values of ΔT for the RB convection.

Stationary and oscillatory instabilities have been comprehensively studied in the RB configuration with a Soret effect [1], [2]. The competition of the two effects in the case of the negative Soret coefficient leads to very interesting time-dependent flow states, i.e., propagating, counter-propagating, standing waves, etc. [3–5]. Stable three-dimensional patterns (rolls, cross rolls, squares) coexist near the onset of instability in the system [6] if the two effects are coaligned.

Here we consider a convection in a binary mixture with a negative Soret effect ($\psi<0$) while the fluid is heated from *above*, i.e., the thermally stable Rayleigh-Benard configuration. La Porta and Surko [7] observed experimentally that the convection amplitude exhibits damped oscillations for a sudden change in the forcing parameters in a similar class of mixtures (water-ethanol) and the same configuration. Recently this regime was extensively studied experimentally in colloidal suspensions [8], [9] and in binary as well as in ternary polymer solutions [10].

Finite amplitude convective oscillations in a binary mixture with a Soret effect were theoretically predicted by Shliomis and Souhar [11]. They argued that in colloidal mixtures with a small particle mobility the concentration gradients sets in so slowly that the Soret convection starts before this gradient reaches its stationary value, i.e., for $\mathrm{Ra}<\mathrm{Ra}^0$, but $\mathrm{Ra}_s>\mathrm{Ra}_s^0$ (for positive ψ and heating from below or negative ψ and heating from above). The increasing convective motion mixes up the fluid, sweeping out the concentration boundary layers and the concentration profile returns to the conductive state since the applied Rayleigh number $\mathrm{Ra}<\mathrm{Ra}^0$, and the process is repeated. They stated that magnetic colloids, with ψ/Le very large [see Eq. (2)], per-

*Electronic address: vshev@ulb.ac.be URL: http://www.ulb.ac.be/polytech/mrc

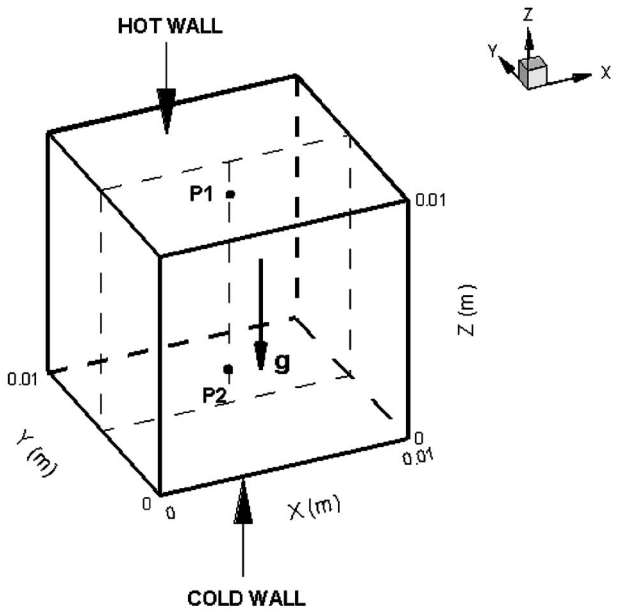

FIG. 1. Geometry of the problem. Time histories are recorded at the two points $P_1=\{x=0.55, y=0.5, z=0.84\}$ and $P_2=\{x=0.55, y=0.5, z=0.12\}$ (dimensionless units).

fectly fit these requirements. Recently, Ryskin *et al.* [3] pointed out that convective perturbations do not decay although $\psi/\mathrm{Le} \gg 1$, hence there is no mechanism that drives the system back to the conductive state.

Present simulations and previous experimental results showed that the convective oscillations predicted by [11] prevail at limited ranges of Rayleigh numbers and during the early stages of Soret-induced convections in liquids with a negative Soret effect (colloidal suspensions, polymer solutions, or water-alcohol mixtures). However self-sustained oscillations have not been demonstrated in any experiment (see [7–10]), although some were performed at very high solutal Rayleigh numbers, e.g., $\psi/\mathrm{Le} \approx 2.7 \times 10^4$. After a few periods of damped oscillations the system usually undergoes a transition to a stationary nonlinear state as predicted by [3].

Here we present a three-dimensional (3D) time-dependent numerical study describing the transient stage of Soret-driven instability in the system heated from above. The previous experiments used a shadowgraph technique, which gave only the total signal summarized over the thickness of the cell. The present calculations allow us to follow the development of the velocity field as well as concentration perturbations.

FORMULATION OF THE PROBLEM

Simulations are performed for a water-isopropanol mixture filling a closed cubic cell, see Fig. 1. The upper and bottom walls are kept at different and constant temperatures T_{hot} and T_{cold}, so $\Delta T = T_{hot} - T_{cold}$. All other walls are assumed thermally insulated. In the case of heating from above the product $g\Delta T < 0$ will be negative thus $\mathrm{Ra} < 0$, while $g\Delta T > 0$ and $(\mathrm{Ra} > 0)$ when heating from below.

Initially the cell is filled with a homogeneous mixture with the mass fraction of the heavier component (water) $C_0 = 0.9$. The parameters of the system correspond to a realistic binary mixture enabling comparison of theoretical predictions with planned experimental studies. The viscosity and the density are $\nu = 1.4 \times 10^{-6}\ \mathrm{m}^2/s$ and $\rho = 984\ \mathrm{kg/m}^3$. Other relevant properties are $\alpha = 1.3 \times 10^{-7}\ \mathrm{m}^2/\mathrm{s}$, $D = 8.7 \times 10^{-10}\ \mathrm{m}^2/s$, $\beta_T = 3.1 \times 10^{-4}\ \mathrm{K}^{-1}$, and $\beta_C = 0.1386$. The size of the cell is $L = 0.01$ m.

The dimensionless nonlinear time-dependent momentum, energy, and mass equations governing the evolution of the system can be written as

$$\frac{\partial \mathbf{v}}{\partial t} + \mathbf{v}\boldsymbol{\nabla}\mathbf{v} = -\nabla p + \nabla^2 \mathbf{v} - \frac{\mathrm{Ra}}{\mathrm{Pr}}(\Theta + \psi c)\mathbf{e}, \tag{4}$$

$$\frac{\partial \Theta}{\partial t} + \mathbf{v}\boldsymbol{\nabla}\Theta = \frac{1}{\mathrm{Pr}}\nabla^2 \Theta, \tag{5}$$

$$\frac{\partial c}{\partial t} + \mathbf{v}\boldsymbol{\nabla} c = \frac{\mathrm{Le}}{\mathrm{Pr}}(\nabla^2 c - \nabla^2 \Theta), \tag{6}$$

$$\boldsymbol{\nabla} \cdot \mathbf{v} = 0. \tag{7}$$

Here $\mathbf{e}$ is the unit vector directed upwards and $\mathrm{Ra} < 0$. The velocity, time, pressure, and temperature scales are, respectively, $V_{ch} = \nu/L$, $t_{ch} = L^2/\nu$, $P_{ch} = \rho_0 V_{ch}^2$, ΔT. The mass fraction is scaled by $c_{ch} = -C_0(1-C_0)S_T \Delta T$.

Boundary conditions include no slip condition for the velocity at the rigid walls $\mathbf{v} = 0$; constant temperatures at the top and bottom while heating from above $\Theta(z=0) = 0$, $\Theta(z=1) = 1$; lateral walls are thermally insulated: $\partial_y \Theta(y = 0, 1) = \partial_x \Theta(x = 0, 1) = 0$. The absence of mass flux at the impermeable rigid walls gives $\partial_n(c - \Theta) = 0$.

Several disparate time scales describe the phenomenon: the viscous time $\tau_\nu = L^2/\nu \approx 70$ s, thermal time $\tau_{th} = L^2/\alpha \approx 770$ s, and diffusion time $\tau_D \approx L^2/D \approx 1.15 \times 10^5$ s.

We use a finite-volume formulation based on an explicit single time step marching method. Convergence and grid independence studies were performed by comparing with benchmark solutions in the case of a pure liquid, see [12].

DISCUSSION

The simulations were performed in a cubic cell with $\mathrm{Pr} = 10.85$, $\mathrm{Le} = 6.7 \times 10^{-3}$, and $\psi = -0.4$, hence, $|\psi/\mathrm{Le}| \approx 60$. Taking into account Eq. (2) our computations were performed in the rather wide range $\mathrm{Ra}_s = 3.26 \times 10^4$ to $\mathrm{Ra}_s = 6.5 \times 10^5$. A finite size cubic cell containing a single fluid transition from the conductive to a single roll convective state is observed at $\mathrm{Ra}^0_{cube} \approx 3500$, see [13]. Here along with the solutal Rayleigh number Ra_s we will also use the reduced Rayleigh number $r = \mathrm{Ra}/\mathrm{Ra}^0_{cube} = \mathrm{Ra}/3500$, which is normalized to the onset of a convection in a pure fluid in a cubic cell. In terms of r our calculations are in the range $0.15 < r < 3.10$.

The evolution of the vertical velocity, temperature, and concentration $\delta C = (C - C_0) \times 10^{-4}$ with time at the points P_1 and P_2 are shown in Fig. 2 for $\mathrm{Ra}_s = 6.5 \times 10^5 (r = 3.1)$. The linear temperature field is established quickly after the temperature difference ΔT is imposed. Due to the negative Soret effect the heavier liquid slowly rises up to the hot wall. The

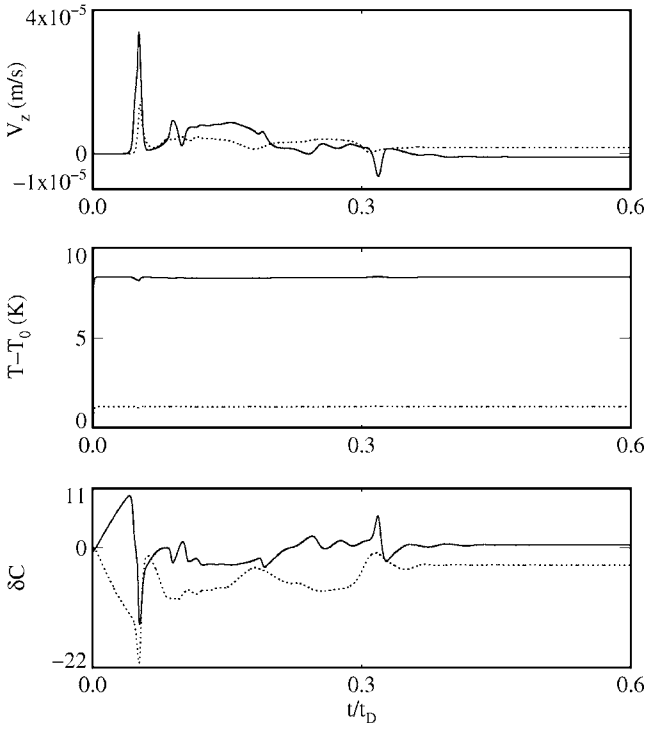

FIG. 2. Time dependence of velocity V_z, temperature, and deviation of concentration from the initial value C_0 at points P_1 (solid line) and P_2 (dotted line); Pr=10.85, $\mathrm{Ra}_s=6.5\times10^5$, and $\mathrm{Ra}/\mathrm{Ra}^0_{cube}=3.1$. Time is measured in a diffusion time scale.

induction period, during which the system remains motionless, $V_z=0$ (upper plot), is significantly smaller than τ_D (by 26), although it lasts *six* τ_{th}. At some moment a strong motion arises then fades; the velocity rises up from zero to a sharp peak at $t=6\times10^3$ s. The heavier liquid is washed away from the hot wall and never achieves the same level later in time. The first splash is followed by a few more pulses of convection, but not as powerful. The temperature field changes visibly only during the first oscillation. At the end of the cycle the temperature and concentration profiles do not tend to functions only of z but rather to functions of all the spatial coordinates. The oscillations are damped out after a few cycles to stationary nonlinear states.

The onset of convection can be characterized by the time required to attain maximal velocity (peak time τ_p). Figure 3 shows this time τ_p as a function of Ra_s. The solid line

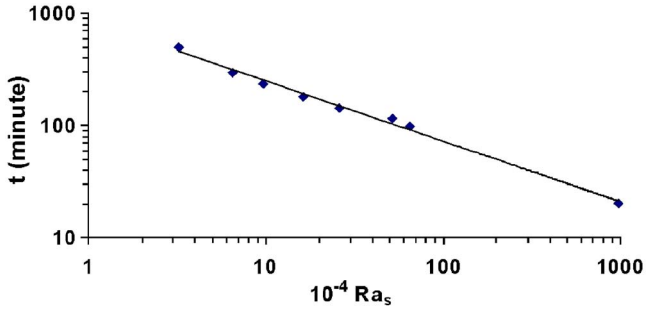

FIG. 3. (Color online) The peak time τ_p as a function of the solutal Rayleigh number. The solid line is the power law fit of all the data $\tau_p\approx1.21\times10^5\ \mathrm{Ra}_s^{-0.52}$.

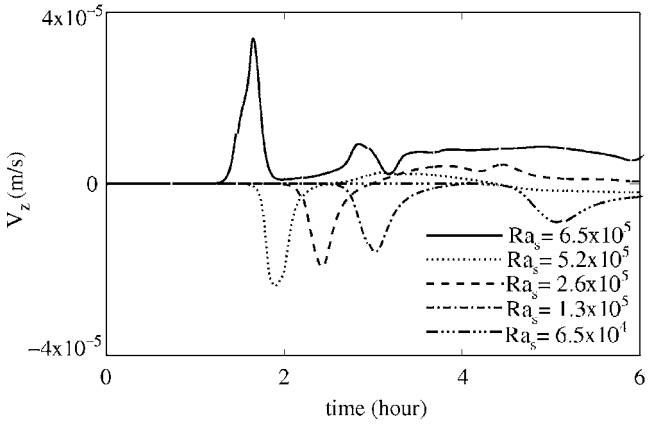

FIG. 4. Temporal evolution of the velocity for different solutal Rayleigh numbers at the point P_1; $6.5\times10^4<\mathrm{Ra}_s<6.5\times10^5$.

represents the fit of the data to the power law $\tau_p\sim\mathrm{Ra}_s^{\gamma}$ yielding the index $\gamma\approx-0.52$. The whole range of examined parameters $0.15<r<3.10$ was used to obtain $\gamma=-0.52$. Taking into account only the first few points when $r<1$ gives $\gamma=-0.43$. These power law fits for $\tau_p(\mathrm{Ra}_s)$ are in very good agreement with theoretical estimates in the limit of a small Lewis number [11] and those measured experimentally in colloids [14]:

$$\tau_p\sim\mathrm{Ra}_s^{\gamma},\quad \gamma=-0.4 \text{ in [11] and } \gamma=-0.52 \text{ in [14]}.$$

The quantitative agreement with experiments is remarkable despite (a) the finite size of our system; (b) the ratio $|\psi/\mathrm{Le}|=60$ vs $|\psi/L|=2.7\times10^4$ in [14]. A comparison of theory [11] with our results as well as [14] is valid only for a limited range of the Rayleigh numbers. Neither our calculations nor the experiments support the theoretically described self-regenerative process.

A shadowgraph technique was used in all relevant experiments [6–9] and the intensity of a signal averaged over the depth of the cell was recorded. This signal had a shape similar to the velocity plot in Fig. 2. Note that the motion starts at P_1 earlier than at P_2 (near a cold wall). The directions of the flows identified from simulations at different Ra_s disclose the interesting temporal flow evolutions shown in Figs. 4 and 5. For $\mathrm{Ra}_s\leqslant5.2\times10^5$, the heavier liquid moves down at the central part of the cell, $V_z<0$ in Fig. 4 during the first pulse. After decay of the first pulsation the damped flow in the central part changes direction (see all broken lines). The damping scenario depends on Ra_s. The situation is opposite for $\mathrm{Ra}_s=6.5\times10^5$ when the cold lighter liquid piles up at the center ($V_z>0$ at P_1) and the hot heavy liquid moves down along the walls.

The mass flux due to the diffusion and Soret effect is $J=-\rho D[\nabla C+S_TC_0(1-C_0)\nabla T]$. In the absence of convection the stationary concentration gradient is proportional to the temperature gradient: $dC/dz=-S_TC_0(1+C_0)dT/dz$ as C and T are uniform in the x,y directions. Amazingly the accumulation of the heavy component follows the same path for different Ra_s (i.e., ΔT). The evolution of concentration δC with time at P_1 for the whole range of Ra_s is shown in Fig. 5 (scaled by factor 10^{-4}). The rate of the component accumulation is the same for all Ra_s, $dc/dt=$const, until convection

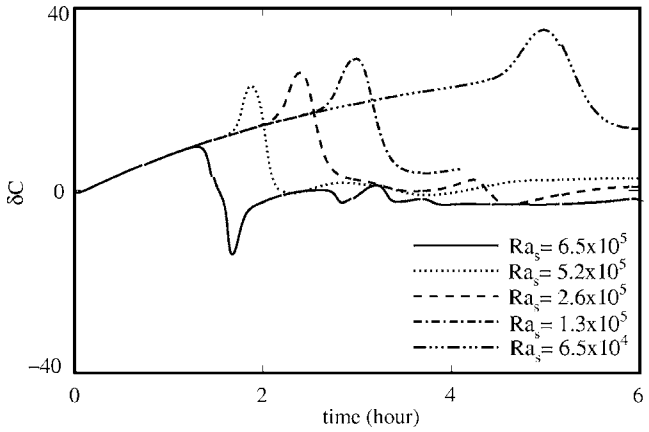

FIG. 5. Evolution of concentration with time at the point P_1 for different solutal Rayleigh numbers $6.5\times10^4<\mathrm{Ra}_s<6.5\times10^5$.

sets in. The smaller the applied temperature difference the longer is the waiting time before the breakdown point. For $\mathrm{Ra}_s\leqslant5.2\times10^5$ the concentration at P_1 sharply increases at the beginning of the convection (see all broken lines). The liquid from the upper hot layer, more rich in the heavy component, moves down and C temporally grows at P_1. While for $\mathrm{Ra}_s=6.5\times10^5$ (solid line) the liquid, poor in C, piles up at the central part. From the beginning of the convection the solid line always lies below the initial profile.

We attribute the change of the direction of the motion to the finite size of the system. Multiple stable steady flow structures have been observed in cubic geometry for the RB convection in a single fluid. For example, the pattern with toroidal structure becomes stable at a reduced Rayleigh number $r=2.83$ for Pr=10, see [13]. This value falls in the range of $2.48<r<3.19$, where the flow pattern changes structure in our system.

The isoconcentration surface shown in Fig. 6 clarifies the flow pattern ($\mathrm{Ra}_s=6.5\times10^5$). The concentration value corresponds to a liquid slightly poor in the heavy component, $c_{0.45}=c_{min}+0.45(c_{max}-c_{min})$. This colder and lighter liquid piles up in the central part of the cell. The occurrence of this columnar (or finger type) convective structure was pointed out in colloid suspensions [8].

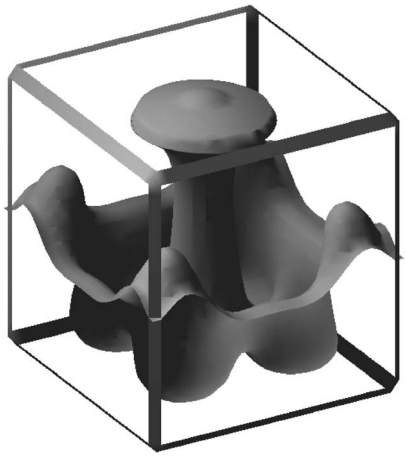

FIG. 6. Snapshot of the isoconcentration surface $c_{0.45}$ at the peak time $\tau_p=1.67$ h, $\mathrm{Ra}_s=6.5\times10^5$.

The convective instability occurs even though the overall density is not adverse as in the usual Benard problem. The gravity dependent terms in Eq. (4) may be written as

$$-\mathbf{g}\beta_T T' + \mathbf{g}\beta_C C' = -\mathbf{g}\beta_T T'[1+\psi]. \tag{8}$$

The expression (8) maintains the same sign because $[1+\psi]>0$. Even for colloid solutions with $\psi\approx-3$ the mechanism seems to be the same. The concentration fluctuations are much more dangerous for instability than thermal fluctuations because of the relatively long life time, $\tau_D\gg\tau_{th}$. Due to the large differences between viscous, thermal, and diffusion times the system has a tendency to fingering buoyant instabilities.

In conclusion we have observed an instability that occurs in a binary mixture with a negative separation ratio while heating from above. The numerical calculations sheds some light on flow structure and the mechanism of instability. The development of Soret-induced convection for water based mixtures in many aspects is similar to those observed in colloidal solutions.

ACKNOWLEDGMENT

The authors wish to thank Professor A. Nepomnyashchy for helpful discussions and advice.

[1] J. K. Platten and J. C. Legros, *Convection in Liquids* (Springer-Verlag, Berlin, 1984).
[2] E. Moses and V. Steinberg, Phys. Rev. Lett. **57**, 2018 (1986).
[3] A. Ryskin, H. W. Müller, and H. Pleiner, Phys. Rev. E **67**, 046302 (2003).
[4] M. C. Cross and P. C. Hohenberg, Rev. Mod. Phys. **65**, 851 (1993).
[5] C. Fütterer and M. Lücke, Phys. Rev. E **65**, 036315 (2002).
[6] B. Huke, M. Lücke, P. Büchel, and Ch. Jung, J. Fluid Mech. **408**, 121 (2000).
[7] A. La Porta and C. M. Surko, Phys. Rev. Lett. **80**, 3759 (1998).
[8] R. Cerbino, A. Vailati, and M. Giglio, Phys. Rev. E **66**, 055301 (2002).
[9] R. Cerbino, S. Mazzoni, A. Vailati, and M. Giglio, Phys. Rev. Lett. **94**, 064501 (2005).
[10] S. Sakurai, Yu Wang, T. Kushiro, T. Nambu, and Sh. Nomura, Chem. Phys. Lett. **348**, 242 (2001).
[11] M. I. Shliomis and M. Souhar, Europhys. Lett. **49**, 55 (2000).
[12] V. M. Shevtsova, D. E. Melnikov, and J. C. Legros, Phys. Rev. E **68**, 066311 (2003).
[13] J. Pallares, F. G. Grau, and F. Giralt, Int. J. Heat Mass Transfer **42**, 753 (1999).
[14] S. Mazzoni, R. Cerbino, D. Brogioli, A. Vailati, and M. Giglio, Math. Control, Signals, Syst. **5**, 305 (2004).